Interplay between bonding and magnetism in the binding of NO to Rh clusters

Prasenjit Ghosh,[1,a)] Raghani Pushpa,[2] Stefano de Gironcoli,[2,3] and Shobhana Narasimhan[1]
[1]*Theoretical Sciences Unit, Jawaharlal Nehru Centre for Advanced Scientific Research, Jakkur, Bangalore 560 064, India*
[2]*International School for Advanced Studies (SISSA), via Beirut 2-4, Trieste 34014, Italy*
[3]*CNR-INFM DEMOCRITOS National Simulation Center, via Beirut 2-4, Trieste 34014, Italy*

(Received 23 July 2007; accepted 1 April 2008; published online 19 May 2008)

We have studied the binding of NO to small Rh clusters, containing one to five atoms, using density functional theory in both spin-polarized and non-spin-polarized forms. We find that NO bonds more strongly to Rh clusters than it does to Rh(100) or Rh(111), suggesting that Rh clusters may be good catalysts for NO reduction. However, binding to NO also quenches the magnetism of the clusters. This (local) effect results in reducing the magnitude of the NO binding energy, and also washes out the clear size-dependent trend observed in the nonmagnetic case. Our results illustrate the competition present between the tendencies to bond and to magnetize, in small clusters.
 [DOI: 10.1063/1.2913242]

I. INTRODUCTION

It is desirable to reduce the NO present in automotive exhaust to N_2, since NO contributes to environmental problems such as ozone layer depletion and acid rain. Of the many precious metals that facilitate the dissociation of the N–O bond (which appears likely to be the rate-limiting step[1–3] in this conversion), Rh appears to be the most efficient catalyst.[4] In general, barriers for such dissociation processes tend to decrease on decreasing the coordination of the metal (catalyst) atoms.[5,6] For example, it has been shown[7–10] that the barrier for NO dissociation is lowered from 0.67 to 0.38–0.46 eV on going from the Rh(111) surface, where surface atoms have ninefold coordination, to the Rh(100) surface, where atoms at the surface have eightfold coordination. [However, Rh(511), which consists of Rh(100) terraces separated by steps, displays a higher barrier for NO reduction than does flat Rh(100), despite being less coordinated.[11]] This raises the question of whether small Rh nanoparticles, which may be expected to have a very high surface-to-volume ratio, and thus a high proportion of undercoordinated sites, may lower the dissociation barrier even further, relative to the value on Rh(100).

There is, however, another factor to be considered: Small Rh clusters are unusual in that they are magnetic, even though bulk rhodium is nonmagnetic.[12–14] At first sight, magnetism might be expected to further enhance the catalytic activity of small Rh clusters: Due to the familiar phenomenon that magnetism tends to increase interatomic distances, magnetic clusters will possess a lower effective coordination, and thus conceivably be better catalysts, than nonmagnetic ones. However, as we will show below, the situation is somewhat more complicated than this: Though reduced coordination favors both bonding and magnetism, the two effects are in competition.

As a first step towards addressing such issues, in this paper we present results from a density functional theory (DFT) study of the binding of NO to very small Rh clusters, where the number of atoms $n \leqslant 5$. These Rh_nNO complexes constitute the initial state for the rate-limiting step in the catalytic reduction of NO. The main motivation of our study is to see how size affects the bonding ability of Rh clusters. The strength of the binding is expected to give an indication of how easy it is to dissociate NO on the Rh_n cluster, since a greater adsorption energy would indicate stronger bonding between the metal atoms and NO, which in turn should result in a weakening of the N–O bond.

The rest of this paper is structured as follows: In Sec. II we summarize previous experimental and theoretical work, both on bare Rh clusters and Rh_nNO complexes. In Sec. III we present some of the technical details of our calculational method. In Sec. IV we present our results, first on the bare Rh clusters, and then on the clusters with NO bound to them. In both cases, we present separately the results of spin-polarized and non-spin-polarized calculations; a comparison of the two enables one to gauge the effects of magnetism. Finally, in Sec. V we summarize and analyze our results and discuss some of their implications.

II. PREVIOUS WORK ON Rh_n AND NO–Rh_n

The possibility that Rh clusters may be magnetic was first suggested by the DFT calculations of Reddy *et al.*,[12] who showed that thirteen-atom clusters of Pd, Rh, and Ru have high magnetic moments. Subsequently, other authors have found other geometries for Rh_{13} that were lower in energy, with a lesser (but nonzero) magnetic moment.[15–18] Extending this work to other sizes, several groups have

[a)]Electronic mail: prasenjit@jncasr.ac.in.

performed calculations to determine the structure, binding energies and magnetic properties of small Rh clusters using DFT as well as other quantum chemical techniques.[15,19–25] There is considerable variation in the structures, binding energies, and spin multiplicities obtained by various authors.

Experimental studies on bare Rh clusters have been carried out by Cox *et al.*[13,14] who found that the clusters do indeed possess rather large magnetic moments, ranging from 0.3 to 1.1μ_B per atom; the magnetic moment per atom decreases with the size of the cluster, becoming zero in the neighborhood of $n=60$. However, the smallest cluster studied by them corresponds to $n=8$. The only experimental work on smaller bare Rh clusters that we are aware of is that of Gingerich *et al.* who studied Rh_2,[26] and determined its binding energy and bond length.

The binding of NO to a Rh dimer has been examined theoretically in a DFT study by Endou *et al.*,[27] who found that the N–O bond length is elongated with respect to its value in the gas phase. There has also been a series of linked experimental and theoretical studies[25,28,29] on the interaction of NO with Rh_6^+ clusters. In their theoretical work, Harding *et al.*[25] found that the energy barrier for NO dissociation on Rh_6^+ ranges from 0.23 to 0.36 eV (depending on the spin state of the cluster), which is markedly lower than the value on the Rh(100) surface.[30]

III. DETAILS OF *AB INITIO* CALCULATIONS

All our DFT calculations have been performed using the PWSCF and PHONON codes, which form a part of the Quantum-ESPRESSO distribution.[31] The Kohn–Sham equations[32] were expanded in a plane-wave basis set with a cutoff of 30 Ry, while a larger cutoff of 216 Ry was used for the augmentation charges introduced by the ultrasoft pseudopotentials[33] that we used to describe the electron-ion interactions. Since the code makes use of periodic boundary conditions, the clusters were placed in a box of side 12 Å; this size is large enough to ensure that the interaction between periodic images is negligible. Accordingly, Brillouin zone integrations were performed using only the Γ point. In order to hasten convergence to self consistency, we have used a very small Gaussian smearing with a width of 0.002 Ry (larger values of the smearing width were found to lead to errors in the magnetic moment of the lowest-energy configuration). Structural stability was verified by determining the vibrational frequencies of the system, using density functional perturbation theory (DFPT);[34] the absence of imaginary frequencies in the vibrational spectrum confirms that the geometries determined by us correspond to true minima in the energy landscape.

Our calculations were performed using both the spin-polarized (SP) and non-spin-polarized (NSP) versions of the Perdew–Burke–Ernzerhof[35] (PBE) form of the generalized gradient approximation (GGA). Though, for magnetic systems, the true ground state corresponds to the result of the SP calculation, a comparison with the NSP calculation (which, by construction, has to yield a nonmagnetic solution) enables one to gauge the effects of magnetization. We note that the SP and NSP calculations can be expected to correctly give the lowest-energy magnetic and nonmagnetic solutions, since these are ground states of different symmetries,[36] thus justifying the validity of the comparison.

As a reference, we have performed calculations on bulk Rh and NO in the gas phase. For the former, we obtain a lattice constant of 3.86 Å and a bulk modulus of 254 GPa, which are in good agreement with the experimental values of 3.80 Å (Ref. 37) and 269 GPa,[37] while for the latter we obtain an N–O bond length of 1.17 Å. This too closely matches the experimentally determined value of 1.15 Å.[38]

In agreement with previous work, we have found that the energy landscapes of the Rh_n and Rh_nNO complexes possess a great many nearly degenerate local minima, both in coordinate space and in spin space. For this reason, we have made use of a very large number of starting configurations (both geometry and spin), and also performed some calculations where the magnetic moment was constrained. We are therefore reasonably confident that we have found the global-minimum structures. Structural optimization was performed using Hellmann–Feynman forces[39,40] and a Broyden-Fletcher-Goldfarb-Shanno (BFGS)-based algorithm[41] for the minimization of energy. Moreover, no symmetry constraints were imposed when performing structural optimization, so as to ensure that distortions were permitted.

For Rh_1 and Rh_2, the question of choosing initial geometric configurations is trivial. For the bare Rh_3 cluster, we tried different triangle-based geometries [equilateral (eq), isosceles (isos), and scalene] as starting configurations. For the initial geometries for Rh_4 and Rh_5, we used the lowest-lying structural isomers reported in the literature:[19–21] The square (sq) and the tetrahedron (tet) geometry for Rh_4 and the triangular bipyramid (tbp) and the square pyramid (sqp) for Rh_5. Further, we made use of a variety of starting spin states; in a few cases we found that it was necessary to constrain the value of the magnetization in order to find some low-lying states.

The situation becomes considerably more complex when considering NO binding to the Rh_n clusters, since there are a large number of inequivalent binding sites, as well as degrees of freedom corresponding to the orientation of the NO molecule relative to the cluster. We have therefore considered a great many starting geometries, and in the majority of cases we found that these relaxed to different local minima of the Rh_nNO complex. The number of inequivalent possibilities that have to be considered increases rapidly as the size of the cluster grows, and it is therefore a rather challenging task to find the global minimum structure.

IV. RESULTS

Though it is well established that small Rh clusters are magnetic, we have performed our calculations both permitting spin polarization (SP) and suppressing it (NSP), since, as discussed above, a comparison of the two can shed some light on the consequences of magnetism. Our results are grouped below into four subsections: (A) Bare clusters+SP, (B) bare clusters+NSP, (C) Rh_nNO+SP, and (D) Rh_nNO +NSP.

A. Bare Rh clusters: Spin polarized

For a single Rh atom, we obtain a ground state that agrees with that which is well-established, both theoretically and experimentally: A ^{4}F ($4d^8 5s^1$) state, with five spin-up ($\uparrow$) and three spin-down ($\downarrow$) electrons in the $4d$ orbital and one $\uparrow$ electron in the $5s$ orbital. This corresponds to a magnetic moment of $3\mu_B$.

For the Rh dimer, we obtain a bond length of 2.25 Å and a binding energy (BE) of 1.48 eV. The former is in excellent agreement with experiment[26] and previous calculations,[21] while the latter closely matches the experimentally reported value of 1.46 eV,[26] as well as some theoretical values.[21] We note that the calculated values for the BE reported in the literature vary over a range, depending on the level of theory used. We obtain a magnetic moment of $2\mu_B$/atom, corresponding to a spin multiplicity ($2S+1$, where S is the total spin of the cluster) of 5. This too is in agreement with earlier experiments and calculations.

There is disagreement in the literature about whether the ground state of Rh_3 is an equilateral triangle with a spin multiplicity of 4,[21] or an isosceles triangle with a spin multiplicity of 6.[20] The lowest energy configuration found by us is in agreement with the latter; it has three nonzero vibrational modes with frequencies of 112.19, 133.28, and 285.61 cm^{-1}. The next-lowest-lying isomer found by us is indeed an equilateral triangle, but its spin multiplicity is 6 and not 4. These two lowest-lying isomers are separated by only 0.008 eV/atom in BE. The equilateral triangle in the quartet spin state lies still higher, by an amount of 0.04 eV/atom.

Low-lying isomers of Rh_4 have either a square or tetrahedral geometry. The lowest-energy configuration found by us corresponds to a tetrahedron with a spin multiplicity of 7; this is in agreement with one set of earlier calculations.[23] Its nonzero vibrational frequencies are found to be 70.87, 138.01, 150.77, 205.45, 210.57, and 284.36 cm^{-1}. We find two energetically degenerate isomers that lie higher than the septet tetrahedron by an amount of 0.05 eV/atom: A square geometry with a spin multiplicity of 5, and a nonmagnetic tetrahedron. We note that some previous studies[12,19,21] have claimed that the latter configuration corresponds to the lowest-energy isomer.

We find two essentially degenerate lowest-energy configurations for Rh_5: Both are square pyramids, one with spin multiplicity of 6, and the other with spin multiplicity of 8. In earlier work, one set of authors had found the former to be the lowest-lying isomer,[19] while another had found the latter.[20] We find that these lie lower than a triangular bipyramid with $2S+1=8$ by a small amount of 0.03 eV/atom. For the square pyramid, with a spin multiplicity of 6, we find the lowest nonzero vibrational frequencies to be 100.55, 144.44, 146.57, 160.09, 176.45, 206.67, 232.60, 233.73, and 288.18 cm^{-1}, respectively, while for the one with a spin multiplicity of 8, we find the lowest nonzero vibrational frequencies to be 45.8542, 94.6457, 133.9002, 134.3358, 182.5663, 230.8963, 236.7408, 236.9311, and 276.2951 cm^{-1}, respectively.

From these results, one can see that even at these very small cluster sizes, there are a large number of nearly degenerate spin and structural isomers, and it seems likely that several isomers will be simultaneously present upon experimentally preparing Rh clusters. We note also that the typical energy differences that we obtain between low-lying isomers are comparable to the error bars in BE that arise from the use of approximate exchange-correlation functionals, which may explain some of the disagreements in the literature about which configuration corresponds to the lowest energy.

As mentioned earlier, we are interested in seeing what effect the coordination number has on reactivity. The nominal coordination number of the lowest-lying isomer increases with the size of the cluster, having values of 0, 1, 2, 3 and 3.2 as n, the number of atoms, is increased from 1 to 5. As expected, as the nominal coordination increases, the interatomic bond lengths increase. Since the effects on electronic structure of increased coordination number and longer bond lengths are expected to be linked and correlated, it is useful to define a quantity that simultaneously incorporates both effects. We therefore define the effective coordination number of the ith atom in a cluster by[42]

$$N_{\mathrm{eff}}(i) = \frac{\sum_{j\neq i}\rho^{\mathrm{at}}_{\mathrm{Rh}}(R_{ij})}{\rho^{\mathrm{at}}_{\mathrm{Rh}}(R_{\mathrm{bulk}})}, \tag{1}$$

where the sum is calculated over all the other atoms j in the cluster, R_{ij} is the distance between atoms i and j, $\rho^{\mathrm{at}}_{\mathrm{Rh}}(R)$ is the computed spherical charge density distribution of an isolated Rh atom at a distance R from the nucleus, and R_{bulk} is the nearest-neighbor bond length in the bulk. In other words, $N_{\mathrm{eff}}(i)$ contains information about the ambient electronic density (due to the other atoms) that the atom i is embedded into. This is in the spirit of the embedded-atom method[43] or effective-medium theory,[44] making the approximation that the density due to the neighboring atoms can be approximated by the sum of the atomic densities. The average effective coordination number of a cluster is then given by $\langle N_{\mathrm{eff}}\rangle = (1/n)\Sigma_i N_{\mathrm{eff}}(i)$.

The filled black circles in Fig. 1 show how $\langle N_{\mathrm{eff}}\rangle$ varies with n for the lowest-lying isomers. It can be seen that the variation is approximately linear, and that $\langle N_{\mathrm{eff}}\rangle$ is significantly larger than the nominal coordination (filled black diamonds).

In Fig. 2, we show the BE and structures of low-lying isomers. (More detailed information, including a comparison with previous calculations, can be found in the supplementary material).[50] Note that both the spin multiplicity and the BE/atom of the lowest-lying isomer also increase monotonically with n, and that the energy difference between the two lowest-lying isomers is indeed minute in all cases. However, we note that the magnetic moment *per atom* decreases monotonically with increasing n, which is in agreement with the expectation that larger clusters, being more highly coordinated, should display a decreased tendency towards magnetization. The filled black circles in Fig. 3(a) show that the binding energy per atom varies more or less smoothly also with $\langle N_{\mathrm{eff}}\rangle$.

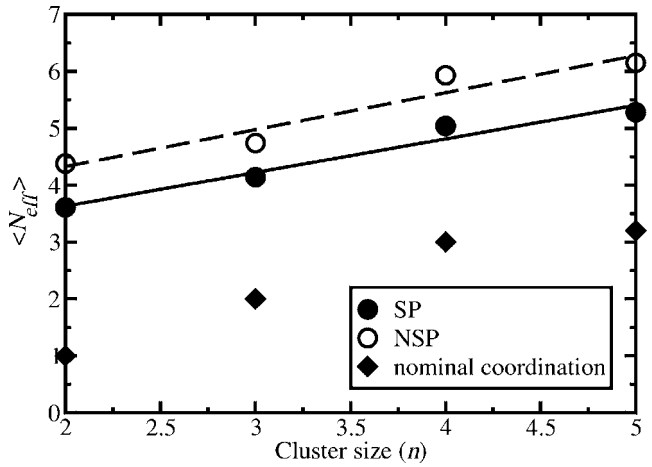

FIG. 1. Effective coordination number ($\langle N_{\text{eff}} \rangle$) vs cluster size ($n$). The filled circles and open circles denote the $\langle N_{\text{eff}} \rangle$ of the clusters for SP and NSP cases, respectively. The filled diamonds show the nominal coordination in each cluster. The solid and the dashed straight lines are guides to the eye for SP and NSP, respectively.

Further details about the geometry, spin state, and energetics of the low-lying isomers found by us, as well as a comparison with earlier results, can be found in Table I of the supplementary information.[50]

B. Bare Rh clusters: Non-spin-polarized

When we repeat our calculations upon constraining the clusters to be nonmagnetic, it becomes immediately obvious that the suppression of magnetism has a noticeable impact on structure: In agreement with general experience, one finds that bond lengths are longer in the SP case than the NSP (details can be found in Table II in Ref. 50). This is because in the SP case, magnetism (which is favored by Hund's rule) is in competition with the tendency to form interatomic bonds; upon suppressing the former, the latter tendency is increased, resulting in shorter interatomic bonds and hence larger values of $\langle N_{\text{eff}} \rangle$ (see the open circles in Fig. 1). While for the SP case, both isosceles and equilateral triangles constitute stable geometries for Rh_3, in the NSP situation, the former relaxes to the latter. We note also that the near degeneracy between the square and tetrahedral structures of Rh_4 appears to be lifted on suppressing spin polarization.

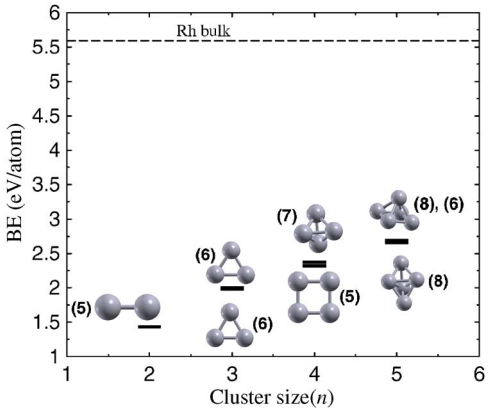

FIG. 2. (Color online) Binding energies vs cluster size (for SP). The horizontal line corresponds to the BE per Rh atom in the bulk. The equilibrium structures of different clusters have been drawn with the spin multiplicity given in parentheses.

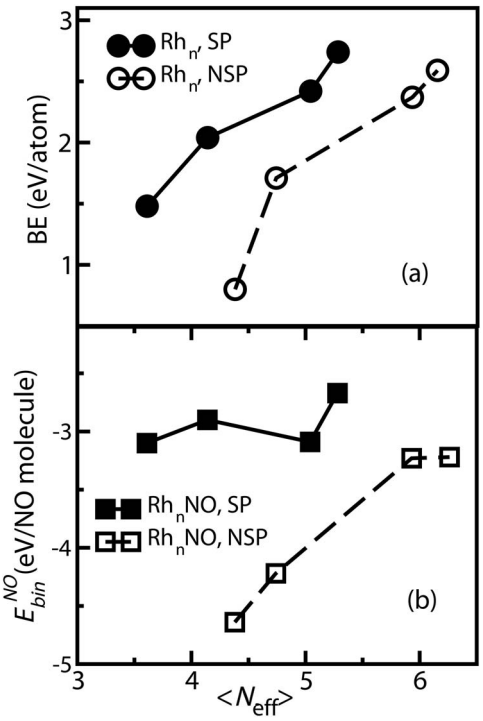

FIG. 3. (a) Binding energy for the bare clusters and (b) NO binding energy vs effective coordination number ($\langle N_{\text{eff}} \rangle$). The filled and open circles show the BEs of Rh_n for SP and NSP, respectively. The filled squares and the open squares denote $E_{\text{bin}}^{\text{NO}}$ for Rh_nNO complexes in SP and NSP cases, respectively.

The open circles in Fig. 3(a) show that the BE varies monotonically with $\langle N_{\text{eff}} \rangle$ also when magnetism is suppressed; this figure makes it clear that allowing magnetism stabilizes the clusters, while decreasing their effective coordination.

C. NO on Rh clusters: Spin Polarized

By considering a variety of starting spin states and geometries, we have found several stable configurations when NO binds to the Rh clusters. The structures of many of these are depicted in Figs. 4–6.

We find that on a single Rh atom, it is most favorable for NO to bind in a "bent" configuration [Fig. 4(a)], while on the Rh dimer, the "vertical bridge" configuration [Fig. 4(c)] is favored. On the Rh trimer, the configuration with lowest energy corresponds to one in which NO sits, perpendicularly, on the hollow site of an equilateral triangle [Fig. 4(k)]. Out of the many possible binding geometries for Rh_4NO depicted in Fig. 5, the one shown in Fig. 5(e) is most optimal, with the nitrogen atom occupying the hollow site on one of the triangular faces of tetrahedral Rh_4, and the molecule being oriented perpendicular to the face. However, the vertical bridge configuration on the tetrahedron [Fig. 5(d)] is very nearly degenerate to this. For the Rh_5NO complex, the most favored geometry is that shown in Fig. 6(g), where NO sits slightly tilted on one of the short edges of the tpb. We note that when Rh_5 is instead in the sqp geometry, the lowest-energy configuration corresponds to Fig. 6(b). Though these two

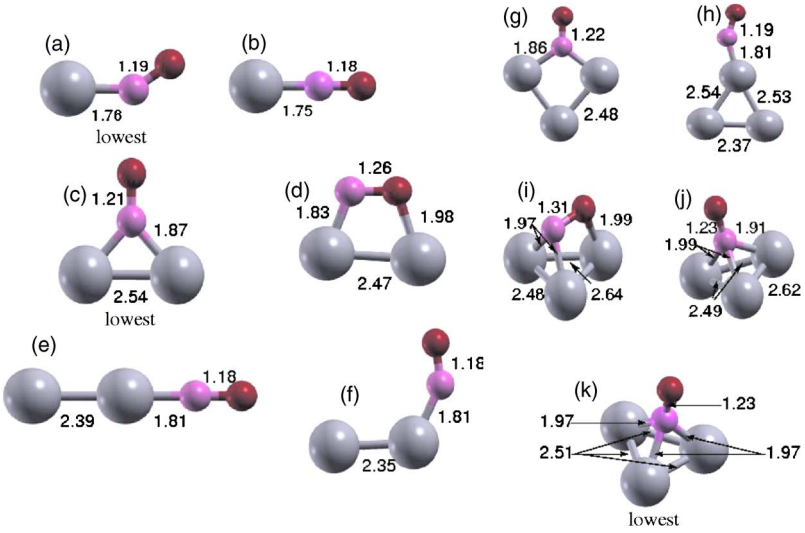

FIG. 4. (Color online) Stable NO binding geometries on Rh_1 [(a) and (b)], Rh_2 [(c)–(f)] and Rh_3 [(g)–(k)] after geometry optimization (for SP cases). The Rh atoms are represented by gray spheres, N atoms by magenta spheres, and oxygen by red spheres. The same color convention has been followed in Figs. 5, 6, and 9. The numbers in the figures are the bond lengths in Å.

configurations differ by 0.14 eV in energy, it is possible that the latter configuration may be stabilized by kinetic barriers, and thus may be observed in experiments. In the rest of the paper we consider the geometry corresponding to Fig. 6(b) as the lowest energy configuration for Rh_5NO.

Note that on Rh_2 and Rh_5, the most favored binding site is a bridge site, while on Rh_3 and Rh_4, it is a hollow site. We attempted to use our results to formulate guidelines for determining binding sites and geometries—for example, by examining bond lengths in the bare clusters and/or looking at the ambient electron density at the binding site, and by comparison with the Rh(100) surface (where NO adsorbs on a bridge site) and the Rh(111) surface (where NO adsorbs in the hexagonal-close-packed hollow site). However, we were not able to determine any clear trends, and thus the problem of determining NO binding sites on larger clusters is likely to require a systematic trial of all possibilities, and thus considerable computational effort.

We define the binding energy of NO on the cluster, $E_{\mathrm{bin}}^{\mathrm{NO}}$, by

$$E_{\mathrm{bin}}^{\mathrm{NO}} = E_{\mathrm{Rh}_n\mathrm{NO}} - E_{\mathrm{Rh}_n^0} - E_{\mathrm{NO}}, \tag{2}$$

where $E_{\mathrm{Rh}_n\mathrm{NO}}$ is the total energy of the Rh_nNO complex, $E_{\mathrm{Rh}_n^0}$ is the total energy of the lowest-lying isomer of the bare Rh_n cluster, and E_{NO} is the total energy of the NO molecule in the gas phase. To avoid any potential confusion, we point out that $E_{\mathrm{bin}}^{\mathrm{NO}}$ is the energy required to separate the Rh_nNO complex into Rh_n and NO, in contrast to the BE discussed in Sec. IV A above, which is the energy required to split up the Rh_n cluster into n isolated Rh atoms.

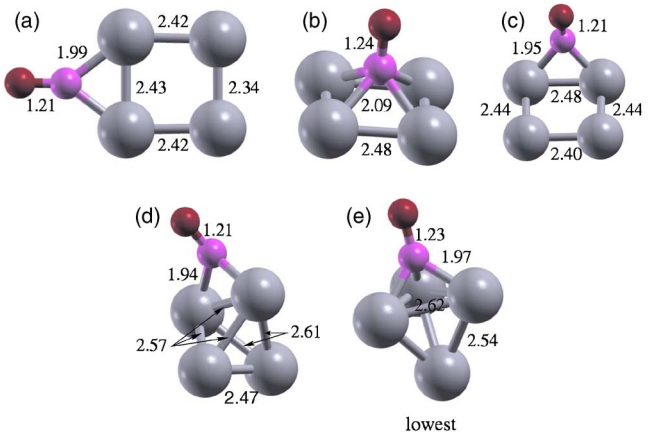

FIG. 5. (Color online) Stable NO binding geometries on Rh_4 after geometry optimization (SP case). The numbers in the figures are the bond lengths in angstroms. See caption to Fig. 4 for color code.

We find that the lowest energy configurations, as one proceeds from $n=1$ to $n=5$, correspond to binding energies $E_{\mathrm{bin}}^{\mathrm{NO}}$ of −3.23, −3.10, −2.90, −3.09, and −2.77 eV, respectively [see also the filled black squares in Figs. 3(b) and 7(a)]. We see that $E_{\mathrm{bin}}^{\mathrm{NO}}$ does not change hugely as a function of cluster size and/or $\langle N_{\mathrm{eff}} \rangle$, though its magnitude is significantly larger on the clusters than on Rh(100) or Rh(111), for which we obtain values[45] of −2.59 and −2.18 eV, respectively.

In Fig. 8, we have shown how the spin multiplicity varies with n, for both the bare clusters and the Rh_nNO complexes. It is clear that in all cases, the effect of NO adsorption is to lower the magnetization significantly—note that in the cases of RhNO and Rh_3NO, the complex is actually found to be nonmagnetic. Upon examining SP charge densities, we find that the magnetism is quenched most strongly for the Rh atoms that are bonded to the NO molecule; the magnetization in the vicinity of other atoms remains either essentially unchanged or, in a few cases, actually increases. As an example, in Fig. 9 we have plotted the *difference* between the ↑ and ↓ densities, for (a) the lowest-energy NO–Rh_5 complex, and (b) the Rh_5 cluster, not in its equilibrium geometry but in the same structure as in (a). A visual inspection of the two figures shows that, in Fig. 9(a), the spin polarization is reduced significantly in the immediate neighborhood of the NO binding site. This becomes even clearer in Fig. 9(c), where we have plotted the difference between (a) and (b), i.e., the change in spin polarized charge density as a result of NO binding. In this figure (in color online), red and blue indicate an increase and decrease, respectively, in the degree of spin polarization. It is very clear that the five atoms of the Rh cluster fall into three groups: (i) In the two Rh atoms bonded to NO the spin polarization decreases (by about 34%), (ii) the next two Rh atoms show a redistribution of spin polarized charge density, with one set of d orbitals

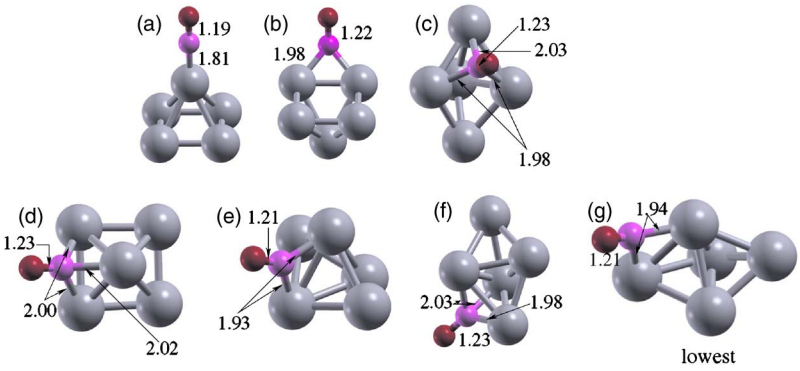

FIG. 6. (Color online) Stable NO binding geometries on Rh_5 after geometry optimization (SP case). The numbers in the figures are the bond lengths in angstroms. See caption to Fig. 4 for color code.

becoming more spin polarized while another set becomes less spin polarized; the overall magnetization for these two atoms does not change significantly, (iii) the remaining Rh atom, which is furthest away from NO, exhibits an increase in spin polarization (by about 13%); this is presumably because its bonds to the other Rh atoms are weakened (as they are now bonded to NO), and it is only in this one atom that the competition between magnetism and bonding is won by the former tendency.

Figures 7(b) and 7(c) show how the N–O distance and the Rh–N distance vary with cluster size. The variation in the former is negligible, and within the limits of accuracy of our calculations. However, we note that, as is to be expected, the N–O bond lengths in Rh_nNO are always larger than in NO in the gas phase. The distance between the Rh and N atoms increases as n increases, possibly indicating a weaker bond between NO and the cluster. The slightly nonmonotonic character of the graph in Fig. 7(c) arises from the fact that the NO adsorption site varies with n: In some cases it is the bridge site, while in others it is instead the hollow site, resulting in slightly longer Rh–N bond lengths.

We have verified that the Rh_nNO complexes we have obtained correspond to minima in the energy landscape, by performing DFPT calculations and checking that no imaginary frequencies are obtained. These calculations also allow us to see how the frequency of the vibrational mode corresponding to the N–O stretch varies with n; these results are plotted in Fig. 7(d). As expected, these values are all lower than the frequency of 1896.54 cm^{-1} obtained in the gas phase, indicating that it is now easier to break the NO bond. Also, again as expected, lower frequencies are obtained when the NO binds at a hollow site than when it binds at a bridge site. We note that the NO frequency gives the curvature of the energy landscape along the degrees of freedom corresponding to an elongation of the NO bond; this frequently correlates with the energy required to break the bond, though it need not necessarily do so.

Details of the numerical values of the geometry, spin state and binding energies for low-lying isomers, as well as Rh(100) and Rh(111), may be found in Table III in Ref. 50.

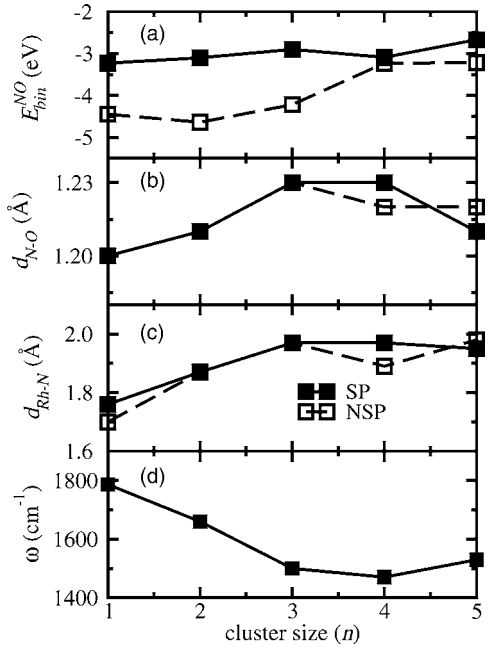

FIG. 7. (a) E_{bin}^{NO} (NO binding energy in eV/NO molecule), (b) N–O bond lengths (d_{N-O}), (c) Rh–N bond lengths (d_{Rh-N}), and (d) the vibrational frequency corresponding (ω) to the N–O stretch for Rh_nNO complexes as a function of n, the number of atoms in the cluster. The filled squares denote the SP results whereas the open squares denote the NSP results.

D. NO on Rh clusters: Non-spin-polarized

The results presented in the three previous sections already hint that magnetism may significantly affect the reactivity of Rh clusters. This becomes clear when we redo our

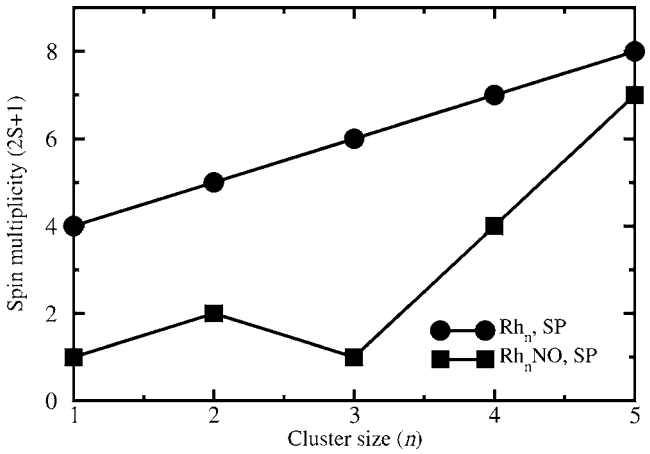

FIG. 8. Spin multiplicity of Rh_n as a function of cluster size, both before (filled circles) and after binding to NO (filled squares).

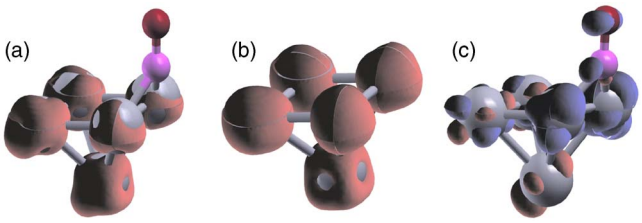

FIG. 9. (Color online) Differences between ↑ and ↓ charge densities ($\delta\rho^s$) of (a) Rh_5NO and (b) Rh_5, but in the same geometry as in Rh_5NO. The difference in $\delta\rho^s$ between (a) and (b) is shown in (c). The red isosurfaces in (c) denote an increase in magnetization and the blue isosurfaces represent a decrease in magnetization. Note the quenching of magnetism in the vicinity of NO in (a), which shows up more clearly in the blue lobes in (c).

calculations of the previous section for the NSP case; numerical results are available in Table IV in (Ref. 50). When magnetism is suppressed, we find that the magnitude of the binding energy $E_{\text{bin}}^{\text{NO}}$ is significantly increased, and now varies monotonically with n, with the binding being most favored on the single Rh atom and least so on Rh_5 [see Fig 7(a)]. The open squares in Fig. 3(b) show how $E_{\text{bin}}^{\text{NO}}$ varies with $\langle N_{\text{eff}}\rangle$ in the NSP case; note the monotonic dependence as well as the difference from the SP situation (filled black squares). It is seen that doing an NSP calculation leads to significantly higher values in the magnitude of the NO binding energy than those obtained upon performing SP calculations.

Looking at the open squares in Figs. 7(b) and 7(c), we see that, in contrast to the behavior of $E_{\text{bin}}^{\text{NO}}$, the N–O and Rh–N bond lengths do not appear to be very sensitive to magnetism (for RhNO and Rh_3NO, the SP and NSP results are identical, since the complexes are nonmagnetic).

V. DISCUSSION AND SUMMARY

We list here the main findings of the previous section: (i) Small Rh clusters are magnetic, as is well established in the literature, (ii) the magnetic moment per atom (for the lowest-energy configuration) decreases monotonically with the size of the cluster, (iii) the average effective coordination number and average bond length both increase as the size of the cluster increases, (iv) as a result of the magnetism of the clusters, the bond lengths increase and effective coordination decreases, relative to what they would be if the clusters were non-magnetic, (v) the NO binding energy $E_{\text{bin}}^{\text{NO}}$ does not display any clear trend as a function of n or $\langle N_{\text{eff}}\rangle$, in the SP case, (vi) however, $E_{\text{bin}}^{\text{NO}}$ is larger (in magnitude) for the clusters than on Rh(100) or Rh(111), (vii) the binding of NO strongly quenches (and, in some cases, eliminates) the magnetization of the bare clusters, (viii) this effect is local, being most prominent on the Rh atoms bonded to the NO molecule, (ix) repeating the calculations with spin polarization suppressed leads to still higher NO binding energies, and (x) we find that the frequency of the vibrational mode corresponding to the N–O stretch is significantly lowered with respect to the gas-phase value, and is lowest for $n=4$.

Our finding that binding of NO is weaker in the magnetic (and less effectively coordinated) case than in the nonmagnetic one may seem, initially, to contradict the general expectation that lower coordination favors increased binding. However, this apparent contradiction arises from the fact that NO binding quenches the magnetism on the Rh clusters. This is similar to what has been observed for CO and NO adsorption on the magnetic Ni(110) surface,[46–48] as well as for NO adsorption on a Rh monolayer in a hypothetical (bulk-truncated) structure.[49] However, in the last of these cases (Ref. 49) we note that the adsorption of NO completely removed the magnetization of the Rh atoms, whereas in our case this effect is only partial. For all the Rh_n and Rh_nNO cases we have examined, the lowest-energy SP solution is lower than the lowest-energy NSP solution (except for RhNO and Rh_4NO, where the two are equal in energy, as the magnetization is totally quenched upon binding to NO). However, the difference in total energy between the NSP and SP Rh_n clusters is much larger than the difference in the total energies of the NSP and SP Rh_nNO complexes, due to the quenching of magnetism in the latter. As a direct consequence of this, the SP binding energies of NO are reduced with respect to the NSP binding energies. Our findings are consistent with those of Nayak *et al.*,[21] who studied Rh_nH_2 clusters, and found that H_2 binds much more strongly to a nonmagnetic isomer of Rh_4 than to a magnetic one.

Thus, lower coordination (which favors binding to gas molecules) also favors magnetism (which disfavors binding to gas molecules). This suggests that for Rh nanocatalysis, there may be an optimally effective cluster size, which is low enough to favor increased binding, while being high enough so that magnetism does not significantly reduce binding. The next step would be to verify whether the greater binding to Rh clusters (relative to flat Rh surfaces) also results in lower barriers for NO dissociation; work in this direction is in progress.

We note that studies of binding such as the ones presented here could conceivably yield four possible indicators of dissociation barriers: (i) The intramolecular (N–O) bond length, (ii) the metal-molecule (Rh–N) bond length, (iii) the NO binding energy $E_{\text{bin}}^{\text{NO}}$, and (iv) the vibrational frequency corresponding to the N–O stretch. One would expect that lowering of dissociation barriers might correlate with an increase in magnitude of (i) and (iii), and a decrease in (ii) and (iv). Of these, it seems likely that (i) will not be a very reliable indicator, given that the N–O distance is almost the same on Rh(100) and Rh(111), even though the dissociation barriers on the two surfaces are different. Indeed, our results show almost no size-dependence for $d_{\text{N–O}}$, in both SP and NSP cases. We find that $d_{\text{Rh–N}}$ decreases as n is decreased, possibly indicating a stronger Rh–N and thus weaker N–O bond. However, the values of $E_{\text{bin}}^{\text{NO}}$ do not show such a size-dependent trend for the SP case. Thus, calculations of dissociation barriers are needed to resolve the issue of whether or not the barriers will vary significantly as a function of size.

Further details of geometries, etc., can be found in the tables submitted to EPAPS.[50]

In conclusion, we find that binding energies for NO are higher on Rh clusters than on Rh surfaces, suggesting that the clusters may be good catalysts for NO reduction. Our results illustrate the fact that in small clusters there can be a competition between the tendencies to bond and to magnetize, with both effects being favored by reduced coordina-

tion. This interplay between bonding and magnetism has a significant influence on the size-dependent trends in the chemical behavior of such systems.

ACKNOWLEDGMENTS

We thank Stefano Baroni for encouraging this collaboration, which was made possibly by a grant from the Indo-Italian Program of Cooperation in Science and Technology 2005-2007, funded by the Department of Science and Technology, Government of India, and the Ministero degli Affari Esteri, Government of Italy. Helpful conversations with Erio Tosatti are acknowledged. We thank Leonardo Gastaldi, Sadhana Relia, and Jimmy Alexander for their assistance. P.G. also acknowledges CSIR, India, for a research scholarship, and S.N. acknowledges the Associateship Programme of the Abdus Salam International Centre for Theoretical Physics, Trieste.

[1] S. B. Schwartz, G. B. Fisher, and L. D. Schmidt, J. Phys. Chem. **92**, 389 (1998).
[2] M. Datė, H. Okuyama, N. Takagi, M. Nishijima, and T. AAruga, Surf. Sci. **350**, 79 (1996).
[3] E. H. G. Backus and A. Eichler, J. Chem. Phys. **121**, 7946 (2004).
[4] D. Loffreda, D. Simon, and P. Sautet, J. Chem. Phys. **108**, 6447 (1998).
[5] T. Zambelli, J. Wintterlin, H. Trost, and G. Ertl, Science **273**, 1688 (1996).
[6] B. Hammer, Phys. Rev. Lett. **83**, 3681 (1999).
[7] H. J. Borg, J. F. C.-J. M. Reijerse, R. A. van Santen, and J. W. Niemantsverdriet, J. Chem. Phys. **101**, 10052 (1994).
[8] M. J. P. Hopstaken and J. W. Niemantsverdriet, J. Vac. Sci. Technol. A **18**, 1503 (2000).
[9] J. S. Villarrubia and W. Ho, J. Chem. Phys. **87**, 750 (1987).
[10] R. M. Wolf, J. W. Bakker, and B. E. Nieuwenhuys, Surf. Sci. **246**, 135 (1991).
[11] D. Loffreda, D. Simon, and P. Sautet, J. Catal. **213**, 211 (2003).
[12] B. V. Reddy, S. N. Khanna, and B. I. Dunlap, Phys. Rev. Lett. **70**, 3323 (1993).
[13] A. J. Cox, J. G. Louderback, and L. A. Bloomfield, Phys. Rev. Lett. **71**, 923 (1993).
[14] A. J. Cox, J. G. Louderback, S. E. Apsel, and L. A. Bloomfield, Phys. Rev. B **49**, 12295 (1993).
[15] Y.-C Bae, H. Osanai, V. Kumar, and Y. Kawazoe, Phys. Rev. B **70**, 195413 (2004).
[16] Y.-C Bae, V. Kumar, H. Osanai, and Y. Kawazoe, Phys. Rev. B **72**, 125427 (2005).
[17] C. M. Chang and M. Y. Chou, Phys. Rev. Lett. **93**, 133401 (2004).
[18] J. Rogan, G. Garcia, C. Loyola, W. Orellana, R. Ramirez, and M. Kiwi, J. Chem. Phys. **125**, 214708 (2006).
[19] T. Futschek, M. Marsman, and J. Hafner, J. Phys.: Condens. Matter **17**, 5927 (2005).
[20] B. V. Reddy, S. K. Nayak, S. N. Khanna, B. K. Rao, and P. Jena, Phys. Rev. B **59**, 5214 (1999).
[21] S. K. Nayak, S. E. Weber, P. Jena, K. Wildberger, R. Zeller, P. H. Dederichs, V. S. Stepanyuk, and W. Hergert, Phys. Rev. B **56**, 8849 (1997).
[22] C.-H. Chien, E. B. Barojas, and M. R. Pederson, Phys. Rev. A **58**, 2196 (1998).
[23] A. Endou, N. Ohashi, K. Yoshizawa, S. Takami, M. Kubo, A. Miyamoto, and E. Broclawik, J. Phys. Chem. B **104**, 5110 (2000).
[24] Y. Jinlong, F. Toigo, and W. Kelin, Phys. Rev. B **50**, 7915 (1994).
[25] D. Harding, S. R. Mackenzie, and T. R. Walsh, J. Phys. Chem. B **110**, 18272 (2006).
[26] K. A. Gingerich and D. L. Cocke, J. Chem. Soc., Chem. Commun. **1** 536 (1972).
[27] A. Endou, R. Yamauchi, M. Kubo, A. Stirling, and A. Miyamoto, Appl. Surf. Sci. **119**, 318 (1997).
[28] M. S. Ford, M. L. Anderson, M. Barrow, D. P. Woodruff, T. Drewello, P. J. Derrick, and S. R. Mackenzie, Phys. Chem. Chem. Phys. **7**, 975 (2005).
[29] M. L. Anderson, M. S. Ford, P. J. Derrick, T. Drewello, D. P. Woodruff, and S. R. Mackenzie, J. Phys. Chem. A **110**, 10992 (2006).
[30] D. Loffreda, F. Delbecq, D. Simon, and P. Sautet, J. Chem. Phys. **115**, 8101 (2001).
[31] http://www.quantum-espresso.org.
[32] W. Kohn and L. J. Sham, Phys. Rev. **140**, A1133 (1965).
[33] D. Vanderbilt, Phys. Rev. B **41**, 7892 (1990).
[34] S. Baroni, S. de Gironcoli, A. Dal Corso, and P. Giannozzi, Rev. Mod. Phys. **73**, 515 (2001).
[35] J. P. Perdew, K. Burke, and M. Ernzerhof, Phys. Rev. Lett. **77**, 3865 (1996).
[36] O. Gunnarson and B. I. Lundqvist, Phys. Rev. B **13**, 4274 (1976).
[37] P. Villars and L. D. Calvert, *Pearson's Handbook of Crystallographic Data for Intermetallic Phases* (American Society for Metals, Metals Park, OH, 1985).
[38] B. G. Johnson, P. M. W. Gill, and J. A. Pople, J. Chem. Phys. **98**, 5612 (1993).
[39] H. Hellmann, (Franz Deuticke, Leipzig, 1937), Sec. 54.
[40] R. P. Feynman, Phys. Rev. **56**, 340 (1939).
[41] C. G. Broyden, J. Inst. Math. Appl. **6**, 76 (1970) R. Fletcher, Comput. J. **13**, 317 (1970) D. Goldfarb, Math. Comput. **24**, 23 (1970) D. F. Shanno, *ibid.* **24**, 647 (1970).
[42] A. Baraldi, L. Bianchettin, E. Vesselli, S. de Gironcoli, S. Lizzit, L. Petaccia, G. Zampieri, G. Comelli, and R. Rosei, New J. Phys. **9**, 143 (2007).
[43] M. S. Daw, S. M. Foiles, and M. I. Baskes, Mater. Sci. Rep. **9**, 251 (1993).
[44] K. W. Jacobsen, J. K. Norskov, and M. J. Puska, Phys. Rev. B **35**, 7423 (1987).
[45] R. Pushpa, P. Ghosh, S. Narasimhan, and S. de Gironcoli (unpublished).
[46] Q. Ge, S. J. Jenkins, and D. A. King, Chem. Phys. Lett. **327**, 125 (2000).
[47] S. J. Jenkins, Q. Ge, and D. A. King, Phys. Rev. B **64**, 012413 (2001).
[48] F. Favot, A. Dal Corso, and A. Baldereschi, Phys. Rev. B **63**, 115416 (2001).
[49] K. C. Hass, M.-H. Tsai, and R. V. Kasowski, Phys. Rev. B **53**, 44 (1996).
[50] See EPAPS Document No. E-JCPSA6-128-804819 for details of the numerical values of geometry, spin states, binding energies of Rh_n and Rh_nNO, both SP and NSP. A comparison with previous calculations and experimental results are also provided where there is available data. For more information on EPAPS, see http://www.aip.org/pubservs/epaps.html.